

Analyzing powers for $^{207}\text{Pb}(\bar{t},p)^{209}\text{Pb}$ at 17 MeV as evidence for multistep contributions

W. W. Daehnick

Nuclear Physics Laboratory, University of Pittsburgh, Pittsburgh, Pennsylvania 15260

Ronald E. Brown, E. R. Flynn, R. A. Hardekopf, and J. C. Peng

Los Alamos National Laboratory, Los Alamos, New Mexico 87545

(Received 29 May 1986)

Analyzing powers and differential cross sections for $^{207}\text{Pb}(\bar{t},p)^{209}\text{Pb}$ have been studied at 17 MeV in order to identify the effects of second-order (\bar{t},p) transfer mechanisms. Angular distributions for transitions to seven single-particle states in ^{209}Pb and to the first pairing vibration state in ^{209}Pb were measured for the angular range $6^\circ \leq \theta \leq 70^\circ$. The observed L dependence of the differential cross sections is adequately reproduced by one-step finite-range distorted-wave Born approximation calculations, but the absolute magnitude of these transitions is underpredicted by factors ranging from 1.25 to 2.5. The analyzing powers for the transitions to the seven well-known single-particle states are significantly different from each other and do not follow one-step distorted-wave Born approximation predictions or any other simple dependence on the transferred angular momentum L . The observed analyzing powers for the $L=5$ transfers to the $\frac{9}{2}^+$ ground state and the $\frac{11}{2}^+$ state at 0.778 MeV differ even in sign. It is found that the inclusion of two-step second-order distorted-wave Born approximation channels, which treat the dominant single-neutron stripping channels as intermediate states, can yield qualitatively correct analyzing powers. In agreement with experiment, two-step calculations predict analyzing powers which depend strongly on the spins (j_1, j_2) of the transferred neutrons. However, quantitatively satisfactory results have only been obtained if an "adiabatic" scattering potential for the intermediate projectile is used. The adiabatic potential, obtained as the sum of a proton and a neutron potential, gives a considerably deeper absorptive part than the empirical deuteron optical model potential. This representation of the intermediate scattering state is supported by a recent two-nucleon transfer model by Austern and Kawai. The inclusion of sequential stripping channels also gives a needed enhancement of the absolute cross sections, although zero-range calculations do not always give quantitatively correct enhancements.

I. INTRODUCTION

Two-nucleon transfer reactions have been used in spectroscopic studies for about 20 years. Their usefulness stems from the observation that direct reaction selection rules tend to be obeyed at all but the lowest energies and from the ability of the distorted-wave Born approximation (DWBA) to correctly account for the observed L dependence of the angular distributions. The familiar selection rules $\Delta T=0$ for (α,d) and (d,α) and $\Delta T=1$ or $\Delta J=\Delta L$ for (t,p) and (p,t) follow from zero-range, one-step transfer theory^{1,2} and have led to many valuable spectroscopic assignments, particularly in the case of strong transitions leading to odd-odd and even-even daughter nuclei. It is of interest and concern that recent two-nucleon transfer work has indicated significant shortcomings of the familiar one-step transfer assumption.

Early on, a number of observed (p,t) transitions that are forbidden in a one-step mechanism were explained by a process of inelastic scattering plus stripping.³ This mechanism generally yields small cross sections, except for deformed targets. However, serious variances from DWBA expectations have also been observed for spherical targets, i.e., for targets near semimagic or doubly magic shells,⁴⁻⁷ and it has been suggested that other two-step mechanisms must be important.⁸ If the analyzing power is one of the

observed parameters, violations of DWBA expectations in two-nucleon transfers are frequent if not typical. They have been reported for (\bar{p},t) as well as (\bar{t},p) reactions.^{9,10} The need for the inclusion of sequential stripping transfer channels has been suggested in many papers and has been supported theoretically,^{8,11,12} but our understanding of this mechanism is still incomplete. A considerable difficulty arises from the fact that two-nucleon transfer calculations are very sensitive to details of the nuclear wave functions and to optical model parameters, as well as to the reaction mechanism. Hence a study with a target that minimizes uncertainties of the nuclear wave functions seems most useful.

To a good approximation ^{207}Pb is a simple $(3p_{1/2})$ -hole target. In the residual nucleus ^{209}Pb , six of the low-lying states are generally regarded as very good single-particle states ($C^2S \approx 1$). Therefore the transfer calculations for $^{207}\text{Pb}(\bar{t},p)^{209}\text{Pb}$ to these states should be free from serious wave function uncertainties or oversimplifications that inevitably affect other analyses. The small number and the simple particle-hole nature of the important intermediate states in ^{208}Pb greatly simplify calculations that aim to include sequential stripping amplitudes. Finally, the ground state of ^{207}Pb has spin $\frac{1}{2}^-$. Since $\Delta S=0$ in the usual perception of (t,p) transfers, this also means that only one L transfer is allowed in the one-step transition.

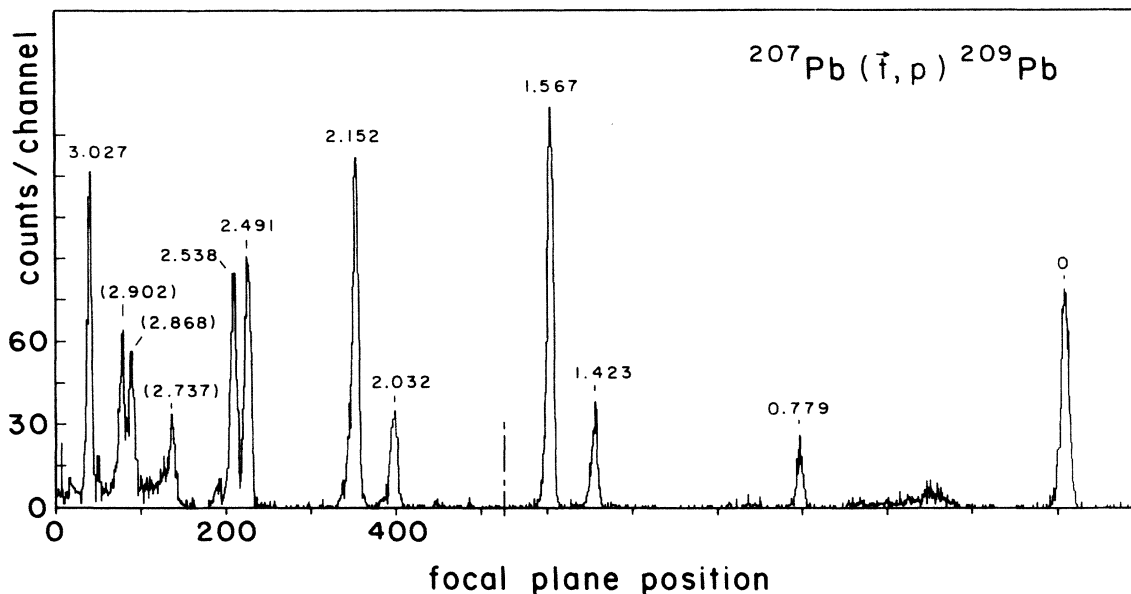


FIG. 1. A $^{207}\text{Pb}(t, p)^{209}\text{Pb}$ pulse height spectrum at 17 MeV observed with a Q3D spectrograph and a position-sensitive helix detector. ^{209}Pb levels are identified by their excitation energy in keV. The experimental resolution is about 19 keV.

Hence the success or failure of the corresponding DWBA or coupled-channels Born approximation (CCBA) analysis must be accounted for almost totally by our degree of understanding of the reaction mechanism. Our $^{207}\text{Pb}(t, p)^{209}\text{Pb}$ study at 17 MeV augments a previously published $^{207}\text{Pb}(t, p)$ experiment with unpolarized tritons of 20 MeV.¹³

II. EXPERIMENT

A. Procedure

The $^{207}\text{Pb}(t, p)^{209}\text{Pb}$ two-particle transfer reaction was studied with a 17 MeV polarized triton beam¹⁴ from the Tandem Van de Graaff at the Ion Beam facility of the Los Alamos National Laboratory. The beam polarization ranged from 75% to 80% and the intensity was about 60 nA. The sign of the polarization was changed at the source and its magnitude was measured by the quench-ratio method¹⁵ before and after each individual spectrum was obtained. Reaction protons were detected in the focal plane of a magnetic quadrupole-dipole-dipole-dipole (Q3D) spectrometer with a helical-delay-line position counter.¹⁶ Beam and target constancy were monitored by detecting elastically scattered tritons with a single Si surface barrier detector located at $\theta=30^\circ$. This angle was chosen because there the elastic analyzing power is very small, $A_p(30^\circ) \leq 0.01$. Measurements of reaction yield, charge integration, and beam polarization were carried out in a computer-controlled sequence and stored on magnetic tape, together with other experimental parameters.

In order to reduce counting rates and background resulting from scattered tritons, the focal plane detector entrance window was covered with a strip of 0.25 mm thick Al foil, which served to stop all tritons; but it only minimally attenuated proton energies. Measurements

were carried out in about 5° intervals between the laboratory angles of 6° and 70° . A 0.97 mg/cm^2 thick isotopically enriched ^{207}Pb target was used. The experimental resolution of about 19 keV was more than adequate to resolve the states of interest. A typical spectrum is shown in Fig. 1.

B. Experimental errors

Particle identification in the Q3D detector was greatly aided by the availability of ΔE , E , and position signals for each event, and their on-line computer analysis.¹⁶ Consequently, the spectra are reasonably free of background, which can be high in triton-induced reactions. The main contaminants in the target were ^{16}O and traces of ^{12}C ; neither presented much trouble in the analysis. The establishment and verification of the absolute cross section scale, however, proved more laborious. In the initial runs the position-sensitive detector in the spectrograph showed substantial losses in the first and the last 20 cm of the 100 cm long detector. This problem disappeared after the helix anode voltage was increased, and a subsequent check found the efficiency along the detector uniform to within statistics (3%). As a further check and precaution, additional data were taken for the known $^{12}\text{C}(t, p)^{14}\text{C}$ and $^{208}\text{Pb}(t, p)^{210}\text{Pb}$ reactions.¹⁷⁻¹⁹ The results were internally consistent and reproducible, but comparison with the well known $^{12}\text{C}(t, p)^{14}\text{C}$ absolute cross sections^{17,18} indicated a product of solid angle and detector efficiency for the Q3D system about 30% smaller than had been expected. The absolute scales given in Fig. 2 therefore rely on a calibration with the results of Refs. 17 and 18, not on the rough scale determination in this experiment. Even with this (higher) normalization the $^{208}\text{Pb}(t, p)$ comparison results still remained 10–20% smaller than the cross sections given in Ref. 19.

We note that the primary objective of this study was

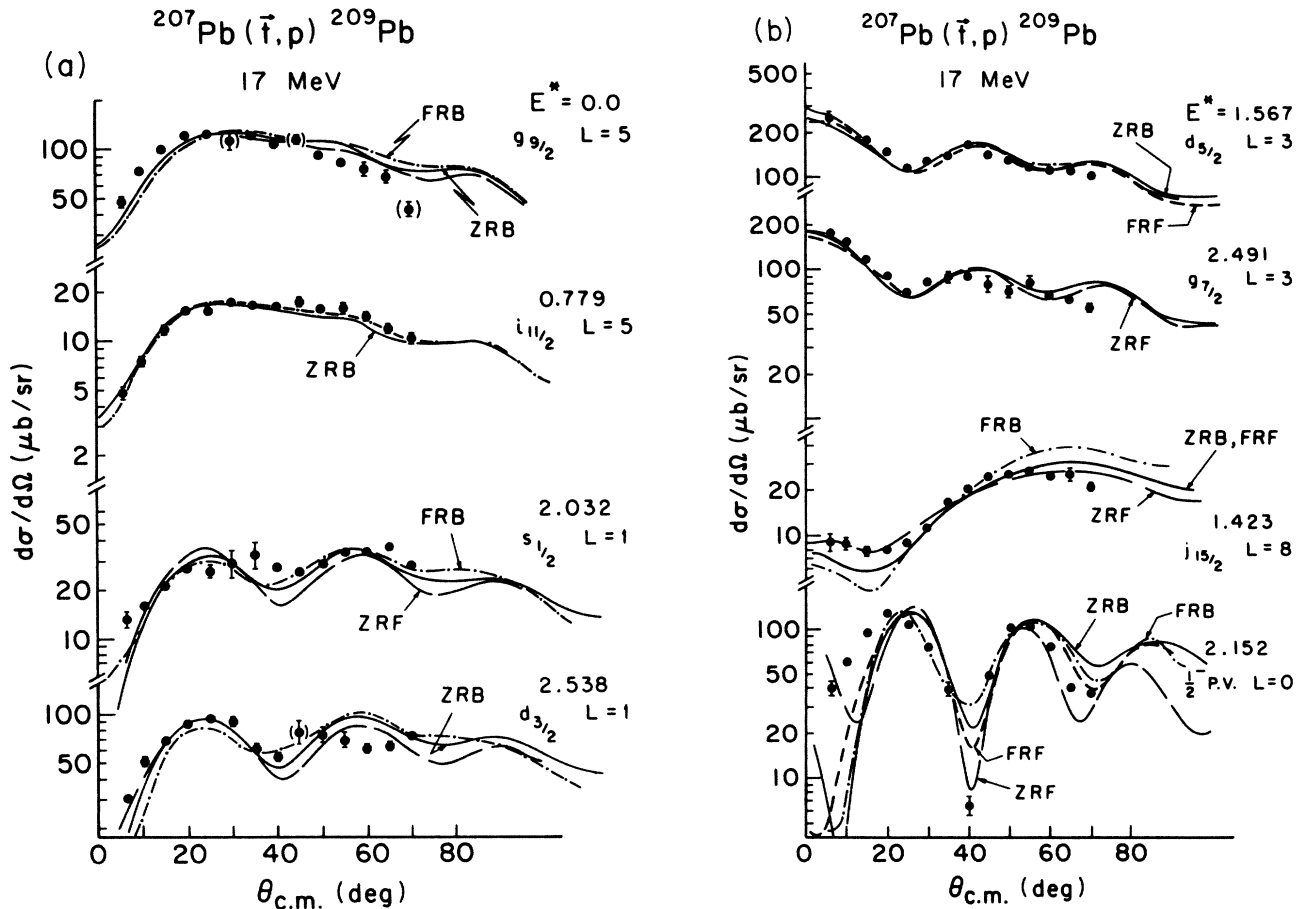


FIG. 2. Differential cross sections for eight well resolved states in ^{209}Pb . The final states are identified by excitation energy (in MeV), L transfer, and l_j or J^π . All curves show one-step DWBA calculations. Four separate curves are shown if they differ sufficiently in shape. The solid lines (labeled ZRB) are zero-range DWBA calculations utilizing BG triton parameters. (The same calculations and parameters are used later for the one-step portion of the CCBA calculations.) The exact finite-range calculations with BG parameters are labeled FRB and shown by dashed-dotted lines; they are sometimes indistinguishable from the ZRB lines. The exact finite range calculations with FL triton parameters, labeled FRF, are shown by short dashes. The FL parameter zero-range curves are labeled ZRF and if different are shown by long dashes.

the measurement of analyzing powers rather than that of absolute cross sections, since a careful spectroscopic study of $^{207}\text{Pb}(\bar{t},p)$ at 20 MeV is available.¹³ We assign a $\pm 20\%$ uncertainty to the absolute cross section scales of the 17 MeV $^{207}\text{Pb}(\bar{t},p)$ data. Random errors resulting from monitoring, background, and dead time uncertainties have been combined with the statistical errors and are shown as error bars in the graphs if they exceed the size of the data symbols. Large error bars usually resulted from the subtraction of poorly resolved impurities. The polarization of the triton beam was found to vary little between measurements. A scale uncertainty of $\pm 2\%$ in the value of the analyzing powers is estimated. This uncertainty is small compared to the random errors mentioned above.

C. Experimental results

The measured cross sections and analyzing powers are shown in Figs. 2 and 3, respectively. The eight transitions analyzed have unique angular momentum transfer, rang-

ing from $L=0$ to 8. There are two transfers each for $L=1, 3,$ and 5 . The pairs of like L show a very strong resemblance in the measured differential cross sections, as was expected from experience and from first order DWBA calculations. However, contrary to DWBA expectations their analyzing powers differ by many standard deviations, and for the $L=5$ pair they differ even in sign. The reaction Q values for the like- L pairs always lie within less than 1 MeV, compared to outgoing projectile energies of 19 MeV. Hence the observed differences ought to be caused primarily by the different microscopic configurations of the transferred neutrons.

III. DWBA CALCULATIONS FOR ONE-STEP TRANSFER

A. Zero range calculations

In the $^{207}\text{Pb}(t,p)^{209}\text{Pb}$ study at 20 MeV an acceptable description of the observed differential cross sections was obtained by zero-range DWBA calculations.¹³ A one-step

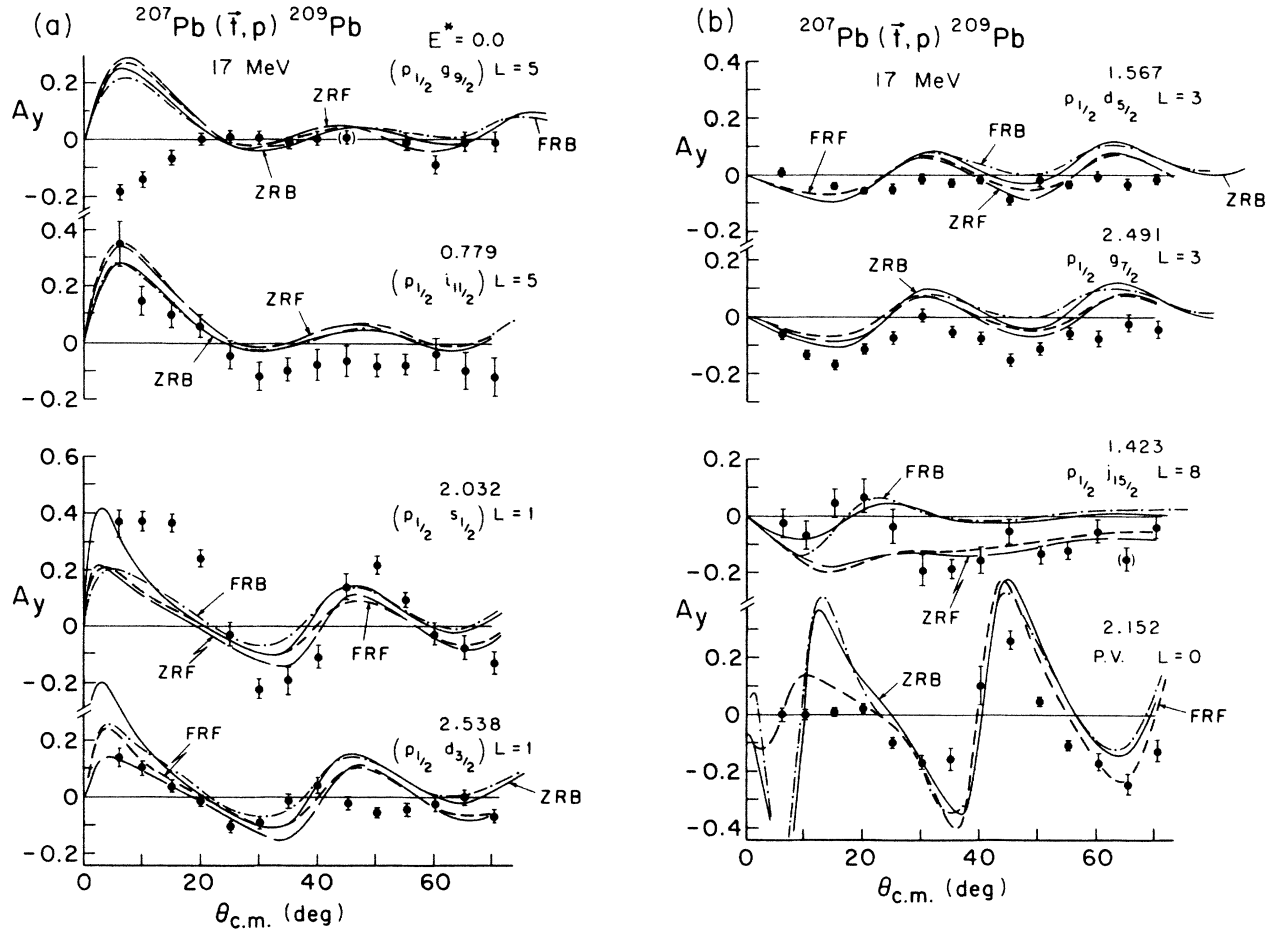


FIG. 3. $^{207}\text{Pb}(\bar{t}, p)^{209}\text{Pb}$ analyzing powers at 17 MeV. For the identification of levels and curves, see the caption of Fig. 2. We note that the use of different triton parameters often produces changes more pronounced than the switch from a zero- to a finite-range treatment.

transfer mechanism was assumed, and the microscopic two-nucleon form factors were calculated following the procedure of Bayman and Kallio.²⁰ The results were used to deduce an average empirical zero-range (ZR) normalization under the (still supportable) assumption that most of the seven single-particle states populated in ^{209}Pb are essentially pure. The empirical ZR normalization factors listed were smallest for the $3s_{1/2}$ state and largest for the $1g_{7/2}$ state, i.e., the extracted normalizations were state dependent and ranged over a factor of 3.3. The normalizations differ even more if the DWBA curves are fitted to the data at their stripping peaks near 20° . In that case the normalizations for the $1g_{9/2}$ and $0i_{11/2}$ states would be higher, and the normalizations would range over a factor of 3.8. In Ref. 13 some deviations were explained in terms of particle-vibration couplings of ^{209}Pb , but in retrospect it seems that in addition to some structure related scatter there is a distinct L dependence.

In corresponding calculations for the present 17 MeV data a similar L dependence for ZR normalizations is found. DWBA calculations were performed with the ZR CHUCK3 code²¹ and with the optical model parameters shown in Table I. CHUCK3 does not compute spectroscopic amplitudes and reordering phases, and they have to be

entered by hand for microscopic (and two-step) calculations. The values used are listed in Table II.

The solid curves in Figs. 2 and 3 present differential cross sections and analyzing powers which were computed with the proton parameters taken from Ref. 22 and with the triton parameter set BG (Bechetti and Greenless).²³ Use of the triton parameter set FL (Ref. 13, Flynn *et al.*) yields cross sections about 1.45 times larger than set BG, but set FL is probably more appropriate for the 20 MeV case, for which it was deduced. If the ZR normalizations are adjusted for best fits to the data as shown in Fig. 2, empirical D_0^2 values from 85×10^4 (for the $s_{1/2}$ state) to 404×10^4 for the $i_{11/2}$ state would be deduced for calculations with potential BG. The "standard" zero-range (t,p) normalization suggested for CHUCK3 is 243×10^4 , and lies in the middle of this range. The standard value for D_0^2 was used for all ZR predictions, unless noted otherwise. As for the 20 MeV results, the range of the renormalizations is large, i.e., 4.7. This range is similar for both sets of triton parameters. For both sets, cross sections for large L are systematically underpredicted, while those for small L are significantly overpredicted with the standard ZR normalization. A detailed listing of the ratio of ZR and finite range (FR) calculations to experiment is given

TABLE I. Typical optical model parameters used in the $^{207}\text{Pb}(t, p)^{209}\text{Pb}$ study. The parameters for protons, deuterons, and those listed as t(BG) are derived from global, energy dependent prescriptions. The entries corresponding to the parameters t(HA) and t(FL) are best fit parameters for the energies indicated. All sets use $r_c = 1.30$ fm. [s.o. denotes spin orbit. The s.o. terms for t(BG) and t(FL) are taken from Ref. 26.]

Projectile	E_L (MeV)	V_0 (MeV)	r_0 (fm)	a_0 (fm)	W_V (MeV)	$4W_D$ (MeV)	r_i (fm)	a_i (fm)	$V_{s.o.}$ (MeV)	$r_{s.o.}$ (fm)	$a_{s.o.}$ (fm)	Ref.
p	19.0	58.6	1.17	0.750	1.48	38.54	1.320	0.660	6.20	1.01	0.75	22
p	17.5	59.1	1.17	0.750	1.15	40.03	1.320	0.661	6.20	1.01	0.75	22
d	18.1	96.0	1.17	0.740	0.41	49.05	1.325	0.905	6.81	1.07	0.66	28
d	13.8	97.1	1.17	0.732	0.24	49.29	1.325	0.905	6.93	1.07	0.66	28
d	12.0	97.6	1.17	0.729	0.18	49.33	1.325	0.905	6.98	1.07	0.66	28
t(BG)	17.0	160.8	1.20	0.720	17.54	0	1.400	0.840	(6.0)	1.10	(0.98)	23
t(HA)	17.0	160.0	1.20	0.660	11.00	0	1.600	1.080	6.00	1.10	0.98	26
t(FL)	20.0	167.5	1.16	0.750	11.29	0	1.500	0.820	(6.0)	1.10	(0.98)	13
"adiabatic" deuteron potentials												
p	6.9					50.63	1.320	0.661				22
p + n	13.8	111.4	1.17	0.750	0.00				6.20	1.01	0.75	22
n	6.9					34.77	1.260	0.580				22
p	6.0					51.53	1.320	0.661				22
p + n	12.0	112.0	1.17	0.750	0.00				6.20	1.01	0.75	22
n	6.0					35.67	1.260	0.580				22

TABLE II. Spectroscopic amplitudes used for the individual channels in the DWBA or CCBA calculations. All amplitudes are calculated for code CHUCK3 under the assumptions that the target is a pure ($3p_{1/2}$) hole in a doubly magic ^{208}Pb shell and that the final states are pure l_j single-particle states outside this core.

Final state (MeV)	l_j	L transfer	$S^{1/2}$ one-step	$S^{1/2}$ two-step intermediate state identification		
				Ground state	$J = j + \frac{1}{2}$	$J = j - \frac{1}{2}$
2.032	$s_{1/2}$	1	-1.225	1.414	-1.225	-0.707
2.538	$d_{3/2}$	1	-0.866	1.414	-1.118	-0.866
1.567	$d_{5/2}$	3	-1.080	1.414	-1.080	-0.913
2.491	$g_{7/2}$	3	-0.935	1.414	-1.061	-0.935
0	$g_{9/2}$	5	-1.049	1.414	-1.049	-0.949
0.779	$i_{11/2}$	5	-0.957	1.414	-1.041	-0.957
1.423 ^a	$j_{15/2}$	8	-1.031	1.414	-1.031	-0.968

^aThis state is treated as a pure $j_{15/2}$ state although it is known to be more complex.

in Table III. Although the model fails to yield accurate absolute cross sections, it is seen in Fig. 2 that the one-step DWBA approach fits the (relative) differential cross sections reasonably well.

In Fig. 3 we show the corresponding one-step DWBA predictions for the analyzing powers. The ZR results for the triton parameter set BG are shown as continuous solid lines. These solid curves also represent the one-step component of the second order DWBA calculations discussed below. The curves for parameter set FL are shown as dashed lines. Except for $L=8$, the curves show only moderate differences. None of the predictions are very close to the observed analyzing powers. Interestingly, we see the most pronounced failures for the subset of transitions that can be classified as ($p_{1/2}$, $j = l + \frac{1}{2}$) transfers. As in some earlier (p,t) work, the one-step zero-range DWBA gives poor predictions for absolute cross sections as well as analyzing powers. Hence the next logical step in this study had to be an application of the microscopic finite-range formalism²⁴ with a realistic (t,p) form factor,²⁵ as is available with the DWBA code FRUCK2.

B. Finite range calculations

A finite-range (t,p) calculation with a realistic form factor like that of Tang and Herndon²⁵ might remove the large normalization uncertainties associated with the ZR treatment of this two-nucleon transfer. This should be especially true for $^{207}\text{Pb}(\bar{t},p)^{209}\text{Pb}$, where both target and residual nucleus have well known wave functions and where good empirical optical model parameters exist. Of course, such a statement implies that the one-step DWBA generates the dominant part of the transition amplitude. Similarly, an expectation of correct predictions for the analyzing powers implies that D -state effects in the triton are small. Both assumptions are open to question, but they should be tested before more complicated reaction mechanisms are invoked.

Some 20 microscopic exact finite-range calculations were performed (with various sets of optical model parameters) and the results are summarized below. As might be concluded from Table III, FR calculations have indeed more predictive power for $^{207}\text{Pb}(t,p)$ than ZR cal-

TABLE III. Comparison of integrated experimental cross sections for various simple states in ^{209}Pb with results of calculations (integrated from 2.5° to 72.5°). The theoretical results are expressed as ratios to the experimental cross sections.

Final state (MeV)	J^π or l_j	L transfer	σ_{expt}^a (μb)	ratios to σ_{expt}			
				$\frac{\sigma_{\text{ZRB}}}{\sigma_{\text{expt}}}$	$\frac{\sigma_{\text{FRB}}}{\sigma_{\text{expt}}}$	$\frac{\sigma_{2 \text{ step}}}{\sigma_{\text{expt}}}$	$\frac{\sigma_{\text{CCBA}}}{\sigma_{\text{expt}}}$
2.152	$\frac{1}{2}^-$	0	294	pairing vibration state			
2.032	$s_{1/2}$	1	128	1.36	0.56	1.95	0.93
2.538	$d_{3/2}$	1	310	0.63	0.48	2.37	3.35
1.567	$d_{5/2}$	3	585	0.70	0.80	1.75	1.04
2.491	$g_{7/2}$	3	342	0.36	0.48	2.71	3.56
0	$g_{9/2}$	5	407	0.46	0.67	1.18	0.79
0.779	$i_{11/2}$	5	63	0.34	0.43	1.11	1.57
1.423 ^b	$j_{15/2}$	8	89	0.23	0.40	1.15	0.88
Average ratio theor./expt.				0.58	0.55	1.75	1.73
Standard deviation				± 0.38	± 0.14	± 0.64	± 1.21

^aThe uncertainty of the summed experimental cross sections is 5–10% and is dominated by detector efficiency corrections.

^bThis state is treated here as a pure $j_{15/2}$ state, although it is known to be more complex (see Ref. 13). According to M. J. Martin, Nuclear Data Sheets 22, 567 (1977), only about 58% of the single-particle strength has been found at this energy (Ref. 27).

culations. The ratios of FR calculations to experiment for the absolute cross sections are more uniform and no longer L dependent. However, many difficulties remain. To begin with, the FR results are as sensitive to optical model parameter details as the ZR approach. For good angular momentum matching ($L=3,5$), all one-step predictions for differential cross sections are very similar, so that in Figs. 2 and 3 sometimes only two of the four predictions could be plotted. The similarities persist for the analyzing powers. However, the calculated cross sections tend to be more sensitive to small differences in the triton parameters than to the use of the ZR approximation. In other words, the FR calculations with the parameter set FL (labeled FRF and shown as dashed curves) are closer to the ZR curves with the same triton parameters (ZRF, long-dashed lines) than to the other FR curves (labeled FRB). This is particularly obvious for the $L=0$ and 8 calculations.

The angular distributions plotted in Figs. 2 and 3 actually understate the severity of optical parameter sensitivity. If a very recent set of triton parameters²⁶ is used (set HA in Table I), all calculated differential cross sections are so severely suppressed at small angles that a normalization to the data becomes difficult. [We believe that the failure of the transfer calculations with this parameter set results from the unusually large imaginary radius and diffuseness parameters. These values were needed for a good fit to the $^{208}\text{Pb}(\bar{t},t)$ analyzing powers at large angles.] This very large effect of what seems like small parameter differences and the absence of theoretically proven criteria for acceptable parameters for distorted waves must create concern. The $^{207}\text{Pb}(\bar{t},p)$ example may be another argument against the use of atypical "best fit" parameters in reaction calculations.

With the parameter set BG, the FR calculation yield typically 55% of the measured cross sections. With (the rejected) parameter set HA, less than 30% of σ_{total} is predicted. Although one might construct a parameter set that yields larger transfer cross sections, the most realistic conclusion seems to be that one-step DWBA predicts only about half of the observed transfer cross section. For $^{207}\text{Pb}(\bar{t},p)$ the one-step DWBA also fails to predict correct analyzing powers. This failure seems especially significant, because the DWBA *systematically* predicts similar analyzing powers for like L , whereas the data show distinctly different patterns (Fig. 3).

IV. CALCULATIONS INCLUDING SEQUENTIAL TRANSFER

The importance of sequential transfer channels for (t,p) transitions to direct-*forbidden* states seems well established. The observations of the preceding section emphasize that not just hindered transfers, but even strong transitions, must have significant higher-order contributions. Although alternative explanations, such as improved finite-range one-step treatments, are still being advocated, their adequacy has been refuted²⁹ for the ($0^+ \rightarrow 3^+$) transitions in $^{208}\text{Pb}(p,t)^{206}\text{Pb}$. Nevertheless, the number of quantitatively successful analyses utilizing the sequential transfer mechanism is still small and further studies are required.

The traditional approach for calculating second order (sequential) terms is a coupled channels Born approximation (CCBA) or a second order DWBA treatment and can be found, e.g., in Ref. 11 or 12. The appropriate expression for sequential transfer terms of the type $A(p,d)C(d,t)B$ is

$$T(\text{pd},\text{dt}) = \int dr^{12} \chi_t^{+*} \langle \psi_t \phi_B | V_{12} + V_{1p} | \phi_d \phi_c \rangle G_d^+ \langle \phi_d \phi_c | V_{2p} | \phi_p \phi_A \rangle \chi_p^- \\ - \int dr^{12} \chi_t^{+*} \langle \psi_t \phi_B | \phi_d \phi_c \rangle \langle \phi_d \phi_c | V_{2p} | \phi_p \phi_A \rangle \chi_p^-, \quad (1)$$

where $G_d^+ = G_d^+(r_d, r_d)$ is the Green's function for the intermediate deuteron channels, and the second integral is the nonorthogonality term. Hashimoto and Kawai,¹² and more recently Igarashi and Kubo,²⁹ have evaluated the $T(\text{pd},\text{dt})$ amplitude in finite range for several realistic triton functions, with special attention to the nonorthogonality term. The success of their calculations is impressive. However, the computational effort needed was large, and some basic assumptions, i.e., that the intermediate state contains a bound or quasibound deuteron, have come under critical scrutiny.³⁰

Lacking access to the extended finite-range computer codes of Ref. 29, we calculated $T(\text{pd},\text{dt})$ in zero range with code CHUCK3. Some shortcomings of the zero-range approach with regard to absolute and relative normalizations were pointed out in Sec. III, and similar difficulties must be expected for ZR two-step calculations. Nevertheless, we did use CHUCK3 in order to obtain at least a quali-

tative test of the importance of the two-step mechanism in this experiment. The nonorthogonality term cannot be computed reliably in ZR, and its effect was approximated by a reduction of the one-step amplitude. Generally, in finite range calculations it had been found significantly smaller than the direct term.¹² Also necessarily omitted were the d -state components of the triton and deuteron wave functions. While these missing refinements have been found very important in direct-*forbidden* transitions, one may speculate that perhaps they are of second order in strong, allowed transitions.

Even with these rough approximations and simplifications the calculations remain complex. Each transition between the (pure) single particle states in ^{207}Pb and ^{209}Pb can proceed via at least four channels. They proceed by the familiar one-step two-neutron transfer and by sequential stripping through the ground state of ^{208}Pb and through (at least) two $(p_{1/2})^{-1}j$ particle-hole states of

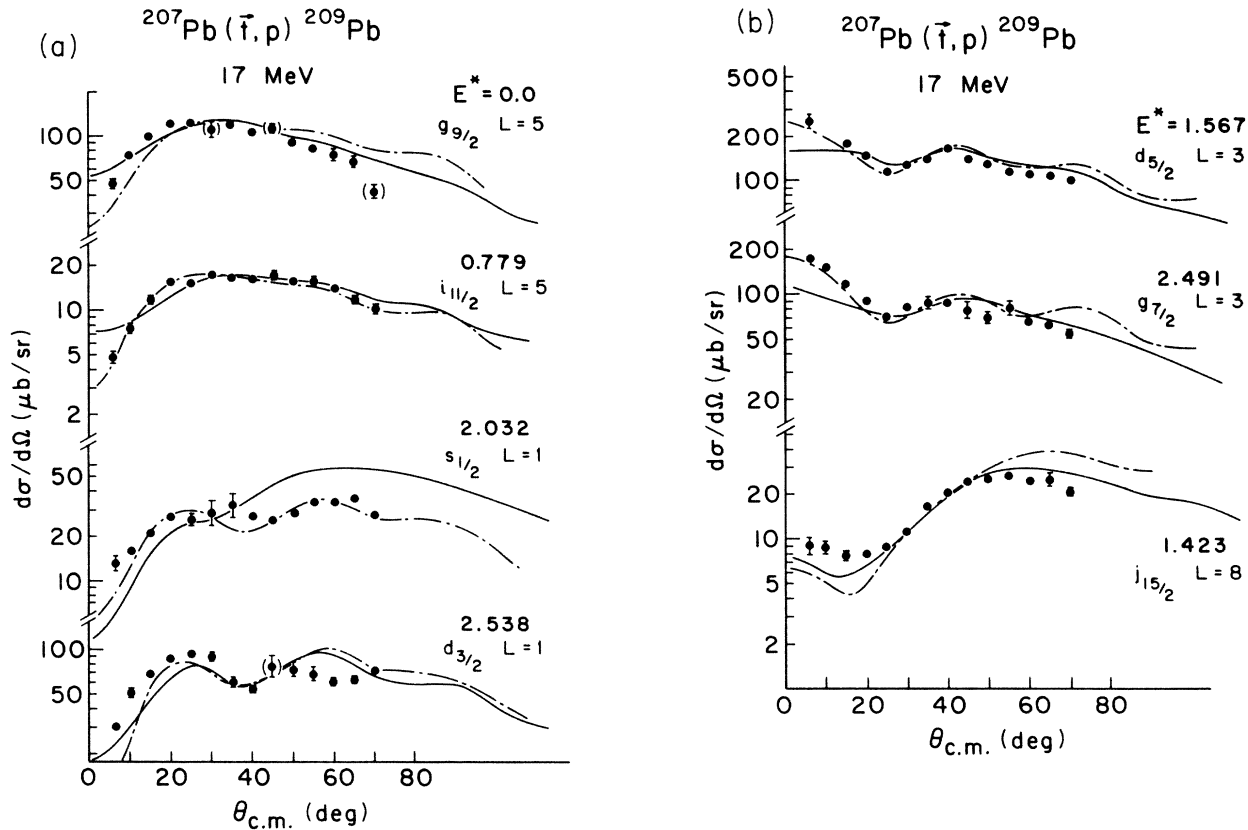


FIG. 4. $^{207}\text{Pb}(\bar{t}, p)^{209}\text{Pb}$ differential cross sections at 17 MeV compared with second order ZR DWBA calculations (solid lines) which include the three dominant sequential transfer (plus the one-step) amplitudes. The dashed-dotted lines represent one-step finite range calculations and are copied from Fig. 2 for reference. The calculations are normalized to the data; the normalization factors are listed in Table III.

^{208}Pb . The spectroscopic amplitudes of each channel for all seven final states of interest are listed in Table II. We note that all factors are of order 1 and hence all amplitudes must be included. In some studies additional two-step channels, e.g., those with the intermediate deuteron in the unbound singlet S state, are considered. The justification for such a *partial* inclusion of the deuteron continuum seems weak.³⁰ Furthermore, test calculations showed that with “reasonable” zero-range normalizations such amplitudes are relatively small. Hence we have omitted singlet terms in the results presented here. (A better treatment of the intermediate deuteron channel has been suggested recently by Austern and Kawai.³⁰)

Before CCBA calculations can be executed, several additional choices remain to be made. The first one is the appropriate ZR normalization for each of the four channels. In the spirit of previous sequential stripping work, the two-step channels were assumed to be parameter free, because the optical parameters used reproduced the single-nucleon transfers on ^{208}Pb very well.³¹ No equivalent predetermination was possible for the ZR one-step amplitude. As discussed above, the cross sections were unreasonably large for low L transfer if the conventional ZR normalization was used. Also, in a more complete calculation, the nonorthogonality term must diminish the one-step term. As a (very rough) first-order guess

we used $\frac{1}{2}$ the recommended ZR normalization ($D_0/2$) for CHUCK3 in our final calculations.

Independent of the particular normalization choices, it is found that the inclusion of two-step channels strongly modifies the computed analyzing powers and absolute cross sections. The L transfer no longer dominates other effects, as in the one-step DWBA. A strong effect of the microscopic structure of the transferred neutron-neutron pair is found, in qualitative agreement with experiment.³²

Nevertheless, as long as we use empirical deuteron optical parameters for the intermediate channels, it remains impossible to explain even approximately the specific changes in the analyzing powers for the $L=1$ and 5 transition pairs. The degree of the difficulty can be seen in Fig. 5(a), where the most striking variances obtained with empirical deuteron parameters are shown as dotted lines. We were finally motivated by Eq. (16) in Ref. 30 to try a different description of the intermediate deuteron, i.e., the so-called adiabatic or Johnson-Soper approximation. Typical empirical and adiabatic deuteron parameters are shown in Table I for comparison. Inspection shows that the summed n and p potentials, while similar to the empirical deuteron potential in their real part, have absorptive terms very much larger than those of a bound deuteron. The use of such strongly absorptive potentials, computed for the appropriate deuteron energy, improves

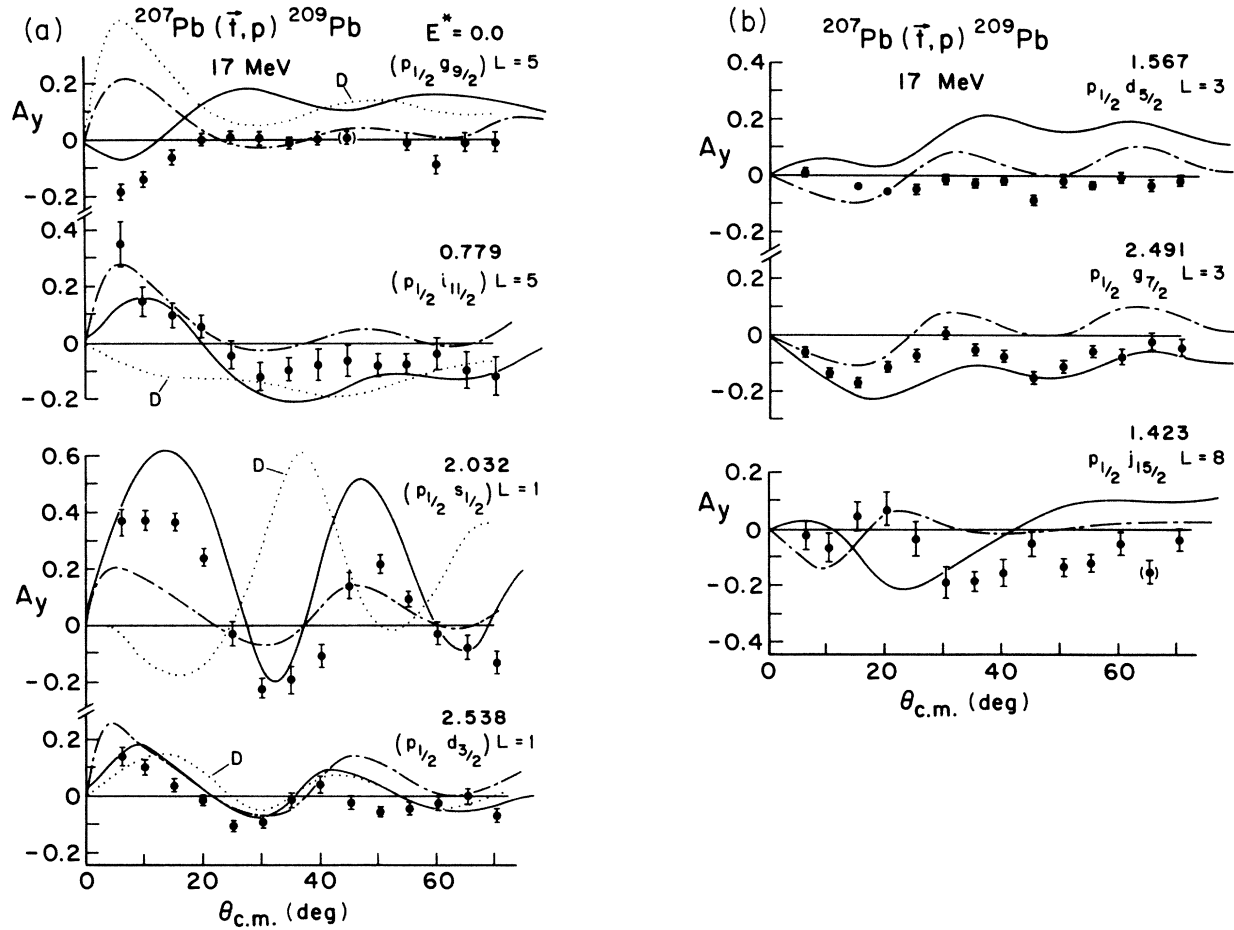


FIG. 5. $^{207}\text{Pb}(\bar{t},p)^{209}\text{Pb}$ analyzing powers at 17 MeV compared with second order ZR DWBA calculations, which include the three dominant sequential stripping transfer channels in addition to the one-step amplitude. The curves shown as solid lines are calculated with adiabatic $(n+p)$ optical model potentials for the intermediate state. The dotted curves (shown only where differences are large) result from identical calculations which utilize (the much less absorptive) empirical deuteron elastic scattering parameters for the intermediate state. The dashed-dotted lines are copied from Fig. 3 for reference only. They represent *one-step* finite range calculations.

the reproduction of the measured analyzing powers. The solid curves shown in Figs. 4 and 5 are CCBA results obtained with adiabatic “deuteron” parameters.

V. DISCUSSION AND CONCLUSIONS

If one were to focus on the fits to the analyzing powers of Fig. 5, one would have to consider the second order DWBA treatment of Sec. IV (solid lines) a striking improvement. The major features of the experimental analyzing powers are reproduced, particularly the configuration dependent changes. (Even better fits can be obtained by assuming L dependent one-step ZR normalizations, but a believable quantitative prescription which corrects for the L dependence of ZR calculations does not exist.) Another success is that the integrated absolute cross sections for five of the seven states now agree to within better than 20% with the data (see Table III, last column).

On the other hand, the transitions to the two highest-lying states ($d_{3/2}$ and $g_{7/2}$) are substantially overpredicted, even more so than with the pure two-step calculation, and the predictions for the differential cross sections, while reasonable, are not as good as those with the one-step FR curves (dashed-dotted lines).

We believe that the ZR approximation and the neglect of an accurate accounting for the nonorthogonality term may be a major cause for the quantitative shortcomings in this second order DWBA treatment of the $^{207}\text{Pb}(\bar{t},p)^{209}\text{Pb}$ reaction at 17 MeV. This belief is strengthened by the even more dramatic failure of the ZR approach in a recent DWBA analysis for the $^{17}\text{O}(\bar{p},t)^{15}\text{O}$ reaction at 90 MeV.³³ It is possible that the approach of Ref. 29 might explain our data quite well, since even our rough ZR approximation had some success. A recalculation with this better code would be most informative.

We recall, however, that the underlying theory in both cases treats the intermediate n - p -nucleus state as a physical deuteron outside the nucleus and essentially neglects

the breakup continuum. If the latter is important, the approach of Austern and Kawai³⁰ should prove to be greatly superior. The important caveat seems to be the strong dependence of our results on the triton and "deuteron" distorted waves. Hence even a superior theoretical approach may not give unique results or may run into some qualitative difficulty. Nevertheless, $^{207}\text{Pb}(\bar{t}, p)^{209}\text{Pb}$ appears to be one of the most suitable cases to test improved transfer theories.

ACKNOWLEDGMENTS

One of us (W.W.D.) wishes to acknowledge helpful conversations with J. R. Comfort and N. Austern. The experimental phase of this work was performed at Los Alamos National Laboratory and supported by the U.S. Department of Energy. The analysis and computing effort was supported by the National Science Foundation and the University of Pittsburgh.

- ¹C. L. Lin and S. Yoshida, *Prog. Theor. Phys.* **32**, 8885 (1964).
²N. K. Glendenning, *Phys. Rev.* **137**, B102 (1965).
³R. J. Ascutto and N. K. Glendenning, *Phys. Rev. C* **2**, 1260 (1970).
⁴W. W. Daehnick and R. Sherr, *Phys. Rev. C* **7**, 150 (1973).
⁵D. K. Olsen, T. Udagawa, and Ronald E. Brown, *Phys. Rev. C* **8**, 609 (1973).
⁶W. A. Lanford and J. B. McGrory, *Phys. Lett.* **45B**, 23 (1973).
⁷J. A. MacDonald, J. Cerny, J. C. Hardy, H. L. Harvey, A. D. Bacher, and G. R. Plattner, *Phys. Rev. C* **9**, 1694 (1974).
⁸N. B. DeTakacsy, *Nucl. Phys.* **A231**, 242 (1974).
⁹K. Yagi *et al.*, *Phys. Rev. Lett.* **40**, 161 (1978).
¹⁰W. P. Alford *et al.*, *Phys. Rev. C* **27**, 1032 (1983).
¹¹W. R. Coker, T. Udagawa, and J. R. Comfort, *Phys. Rev. C* **10**, 1130 (1974).
¹²N. Hashimoto and M. Kawai, *Phys. Rev. Lett.* **59B**, 223 (1975); *Prog. Theor. Phys.* **59**, 1245 (1978).
¹³E. R. Flynn *et al.*, *Phys. Rev. C* **3**, 2371 (1971).
¹⁴R. A. Hardekopf, in *Proceedings of the Fourth International Conference on Polarization Phenomena in Nuclear Reactions, Zürich (1975)*, edited by W. E. Gruebler and V. Konig (Birkhauser, Basel, 1976), p. 865.
¹⁵R. A. Hardekopf *et al.*, *Phys. Rev. C* **13**, 2127 (1976).
¹⁶E. R. Flynn, S. Orbeson, J. D. Sherman, J. W. Sunier, and R. Woods, *Nucl. Instrum. Methods* **128**, 35 (1975).
¹⁷P. W. Keaton *et al.*, *Nucl. Phys.* **A179**, 561 (1972).
¹⁸S. Mordechai *et al.*, *Nucl. Phys.* **A301**, 463 (1978).
¹⁹E. R. Flynn, R. A. Hardekopf, J. D. Sherman, and J. W. Sunier, *Phys. Lett.* **61B**, 433 (1976).
²⁰B. F. Bayman and A. Kallio, *Phys. Rev.* **156**, 1121 (1967).
²¹The coupled reaction channels program CHUCK was written by P. D. Kunz, University of Colorado. His version CHUCK2 was expanded in Pittsburgh by J. R. Comfort and named CHUCK3 (unpublished).
²²F. D. Becchetti and G. W. Greenlees, *Phys. Rev.* **182**, 1190 (1969).
²³F. D. Becchetti and G. W. Greenlees, in *Proceedings of the Third International Symposium on Polarization Phenomena in Nuclear Reactions, Madison, Wisconsin*, edited by H. H. Barschall and W. Haerberli (University of Wisconsin Press, Madison, 1971), p. 682.
²⁴The finite range DWBA code FRUCK2 was written by P. D. Kunz, University of Colorado (unpublished).
²⁵Y. C. Tang and R. C. Herndon, *Phys. Lett.* **18**, 42 (1965); Y. C. Tang, E. W. Schmid, and R. C. Herndon, *Nucl. Phys.* **65**, 203 (1965).
²⁶R. A. Hardekopf *et al.*, *Phys. Rev. C* **21**, 906 (1980).
²⁷M. J. Martin, *Nuclear Data Sheets* **22**, 567 (1977).
²⁸W. W. Daehnick, J. D. Childs, and Z. Vrcelj, *Phys. Rev. C* **21**, 2253 (1980).
²⁹M. Igarashi and K.-I. Kubo, *Phys. Rev. C* **25**, 2144 (1982).
³⁰N. Austern and M. Kawai, *Phys. Rev. C* **31**, 1083 (1985).
³¹W. W. Daehnick, M. J. Spisak, and J. R. Comfort, *Phys. Rev. C* **23**, 1906 (1981).
³²W. W. Daehnick, Ronald E. Brown, E. R. Flynn, R. A. Hardekopf, and J. C. Peng, in *Proceedings of the International Conference on Nuclear Structure*, edited by A. van der Woude and B. J. Verhaar (European Physical Society, Amsterdam, 1982), Vol. 1, p. 278.
³³K. F. von Reden, W. W. Daehnick, S. A. Dytman, R. D. Rosa, J. D. Brown, C. C. Foster, W. W. Jacobs, and J. R. Comfort, *Phys. Rev. C* **32**, 1465 (1985).